Facile synthesis of a mixed matrix membrane based on PTA@MOF-199 nanoparticles with proton conductivity

H. Guo[a,#], J. J. Zhang[b,#], J. H. Liu[a], S. J. Fan[a,*]
[a]*Research Institute of Medicine and Pharmacy, Qiqihar Medical University, China*
[b]*Department of Neurology, Qiqihar First Hospital, China*

Firstly, $H_3[P(W_3O_{10})_4]$@MOF-199 nanoparticles (PTA@MOF-199) of uniform morphology, about 80-125 nm, were successfully synthesized by a simple one-step reaction under solvothermal conditions and then these as-prepared nanoparticles were incorporated into polyvinyl alcohol (PVA) and polyvinyl pyrrolidone (PVP) with solution-cast technique to fabricate a series of proton-conducting mixed matrix membranes with different mass percentage of PTA@MOF-199. These membranes were characterized by XRD and FT-IR. Afterwards, the influence of the mass percentage of PTA@MOF-199 and temperature on the proton-conducting properties were evaluated. Our work confirmed that the polyoxometalate (POM) functionalized MOFs had great application potential as proton conductive materials and provided a basis for further studies on other POM@MOFs based proton-conducting membranes fabrication.

(Received April 4, 2023; Accepted June 3, 2023)

Keywords: MOF-199, Phosphotungstic acid, Proton conduction membranes, Fuel cells

1. Introduction

Proton exchange membrane fuel cells (PEMFC) are widely regarded as promising and efficient energy devices due to their high efficiency, high energy density and pollution-free characteristics [1]. The proton conduction membranes (PEM) are the heart of the proton exchange membrane fuel cells. PEMs are thin membranes with ion-selective permeability, which are solid electrolytes with a polymer structure, also known as an ionic conductive polymer. PEMs should not only separate the fuel and oxidant to avoid direct contact, but also assume the function of conducting protons, and their features will directly affect the output performance, energy conversion efficiency and service life of proton exchange membrane fuel cells [2-4]. The ideal proton conduction membranes should have excellent proton conduction performance and good chemistry and thermal stability to ensure the fuel cell to keep a relatively low ohmic impedance at higher currents. Researches on PEMs have been carried out since the early 1960s, but until now there has been only the perfluorosulfonic acid membrane commercially available [5-7]. Although the perfluorosulfonic acid membrane has high proton conductivity, good chemical and mechanical stability, its high cost, poor proton conductivity at medium temperature and high methanol

* Corresponding author: fansongjie@qmu.edu.cn
https://doi.org/10.15251/DJNB.2023.182.727
#These authors contributed equally to this work

permeability limit its large-scale promotion and application [8]. So, exploiting higher proton conducting and lower-cost membrane materials is the most important task to promote the efficiency of the PEMFCs.

Metal-organic framework materials (MOFs) are another important porous material after zeolite and carbon nanotubes that have developed very rapidly in recent years. MOFs compose of metals (single-metal ions or metal clusters) connected by organic linker to form a three-dimensional crystal structure. Due to the high surface area, adjustable pore sizes, regular void cages, tunable surface properties and easy functionalization, MOFs have shown broad application prospects in the fields of catalysis [9], energy storage[10] and gas separation[11],etc. In recent years, many research reports have shown that MOFs are expected to become a new type of proton conduction membrane material [12-15]. Meanwhile, the mixed matrix membranes of MOFs make it possible for them to be used for industrial applications. However, most MOFs materials are not stable in aqueous or acidic solutions. Therefore, there are very few MOFs that could be practically selected as proton conduction membrane materials.

MOF-199 (an abbreviation of copper (II) benzene-1, 3, 5-tricarboxylate) shows good structural stability against aqueous HCl (pH = 1), aqueous NaOH (pH = 14), water (at 373 K for 4 h) or exposure to 90% relative humidity at 300 K for 28 days [16]. So, MOF-199 could be selected as a promising candidate for proton conduction membrane fabrication. Another challenge is how to improve the proton conductivity of MOF-199. The most generally used method to promote the proton conductivity of MOFs is encapsulation of guest molecules in the channels of MOFs, such as imidazole [17], triazole [18] hydronium ions [19], or histamine [20],etc. The embedded guest entities not only can be used as proton carriers, but also can form a hydrogen bonding network for proton transfer [21]. Recently, we prepared uniform PTA@MOF-199 nanoparticles by a simple one-step reaction under solvothermal conditions to be used as a selective cationic dye adsorbent [22]. PTA@MOF-199 is constructed from Keggin-type heteropolyacid of phosphotungstic acid (PTA, $H_3[P(W_3O_{10})_4]$) integrated into the host material of $Cu_3(BTC)_2$ (MOF-199) to form a three dimensional MOF material [23]. PTA as a typical polyoxometalate (POM), consisted of P, W metal oxygen clusters in nanoscale to form P-W anions, which are balanced by cations. The charged cations can be varied from light metal, organic ammonium, as well as protons [24]. The protonic POMs have been widely applied in proton-conducting devices due to the high proton transfer/storage abilities [25].

In addition, the fabrication of MOF membranes is considered as a crucial step for successful utilization of MOF materials for proton-conducting application. Proton-conducting mixed matrix membranes (PC-MMMs) are composed of a polymeric matrix in which functional particles are embedded. PC-MMMs combine the advantages of dispersed material (e.g., thermal, water and acid stability) and the host polymers (e.g., formability and ionic conductivity). Due to the flexible selection of dispersed and matrix materials, PC-MMMs were viewed as uniquely suitable for addressing traditional PEM challenges [8].

Based on the above considerations, our main objective of the present work is introducing proton conductivity in MOF-199 with PTA from host-guest chemistry concept, and developing a synthesis method for preparing PC-MMMs with lower cost and higher performance based on PTA@MOF-199 NPs with polyvinyl alcohol (PVA) and polyvinyl pyrrolidone (PVP) as substrates. As far as we know, there are few examples on reporting the fabrication of polyoxometalate-based MOFs composites membranes or films and their proton conductivity properties. This work

contributes to drive the further blossom of the proton conduction membranes with polyoxometalate-based MOFs composites in the future.

2. Experimental

2.1. Material

Copper acetate ($C_4H_6CuO_4 \cdot H_2O$, 99%, Tianjin Tianli Chemical Reagent Co. LTD), anhydrous alcohol (95%) and 1,3,5-benzenetricarboxylic acid (trimesic acid, H_3BTC, 98%, Guangzhou Weibo Chemical Co. LTD) were used to prepare MOF-199. Phosphotungstic acid ($H_3[P(W_3O_{10})_4] \cdot XH_2O$, Shanghai Yuanye Biotechnology Co., Ltd, AR, 99%), PVA (Tianjin Guangfu Fine Chemical Research Institute,AR,99%) and PVP (Tianjin Guangfu Fine Chemical Research Institute,AR,99%)were all used as received.

2.2. Syntheses of PTA@MOF-199

The PTA@MOF-199 NPs was prepared according to our previous report with very little modification [22]. Briefly, 0.502 g copper acetate and 0.8 g PTA were dissolved in 10mL water making mixture 1. Then the mixture 1 was added to mixture 2 (a solution of 10mL anhydrous alcohol with 0.583g H_3BTC) to get the mother solution which was stirred under room temperature for 2h followed by centrifugation. Afterwards the obtained blue powder was thoroughly washed three times with deionized water and anhydrous alcohol under ultrasonication respectively.

2.3. Membranes preparation

Firstly, PVA (10 g) and 90 mL of distilled water were added into a flask and dissolved at room temperature for 10-12 h. Then the reaction mixture was kept at 90 °C for 2 h in the reflux device to prepare PVA colloid (10%Wt.%). To prepare the PVP colloid (20%Wt.%), PVP (10 g) was dissolved in 40mL of distilled water and kept at room temperature for 30min.

Then with the “solution-cast” technique, PTA@MOF-199 incorporated polymeric matrix membranes were fabricated. Different amounts of PTA@MOF-199 NPs were dispersed into the PVA and PVP colloid. Afterwards, the mixture was poured into plastic Petri dishes and allowed to evaporate slowly at ambient condition to form the desired hybrid membranes. The fabricated hybrid membranes were denoted as PTA@MOF-199-PVA-X (X=5%、10%、20%、30%、50% Wt.%), PTA@MOF-199-PVP-X (X=5%、10%、20%、30%、50% Wt.%).

2.4. Proton conductivity measurements

Proton conductivity (PC) of the samples was explored using the AC impedance spectroscopy method. The resistance was measured by using an impedance analyzer (PARSTAT 4000, Princeton Applied Research) with an oscillating voltage of 0.1 V over a frequency range of 0.1 Hz to 1.0 MHz. The samples were fully hydrated in 98% relative humidities (RH) for 3 days prior to testing. The temperature was recorded in close proximity to the membrane with a K-type thermocouple in order to measure the temperature dependence of the conductivity. The resistances were extracted from the semicircles of the Nyquist plots directly. PC (σ, S cm^{-1}) was calculated as the follow equation (1):

$$\sigma = \frac{L}{RA} \tag{1}$$

where L (cm) and A (cm^2) are the thickness and area of the membranes, and R(Ω) is the bulk resistance of the samples.

2.5. Characterization

X-ray diffraction (XRD) patterns were performed on a Siemens D5005 diffractometer using Cu kα radiation (λ = 1.5418 Å，150mA and 40KV) with a scanning rate of 4° min^{-1} in the 2θ range from 4 to 40°. A NicoLet Impat 410 FTIR spectrometer was used to collected the Fourier transform infrared spectra (FT-IR) at room temperature in the range of 400-4000 cm^{-1}, with potassium bromide pellets. The morphologies of the material were observed by field-emission scanning electron microscopy (FE-SEM, Shanghai Shangtian Precision Instrument Co., LTD). The resistance was measured by using an impedance analyzer (PARSTAT 4000, Princeton Applied Research) with an oscillating voltage of 0.1 V over a frequency range of 0.1 Hz to 1.0 MHz.

3. Results and discussions

3.1. Characterization results

Powder XRD patterns of simulated MOF-199, PTA@MOF-199-PVA-X and PTA@MOF-199-PVP-X (X=5%、10%、20%、30%、50% Wt.% respectively) were displayed in figure 1. Overall, all the diffraction peaks match well with the simulated MOF-199 diffractogram indicating the good preservation of the crystallinity of the MOF-199 network in the process of PTA encapsulation and the combination with the two kinds of polymeric matrix materials. Moreover, the X-ray signal of PTA@MOF-199-PVP-X is stronger than that of PTA@MOF-199-PVA-X at all the same concentrations, and the overall spectral lines tend to be much smoother correspondingly.

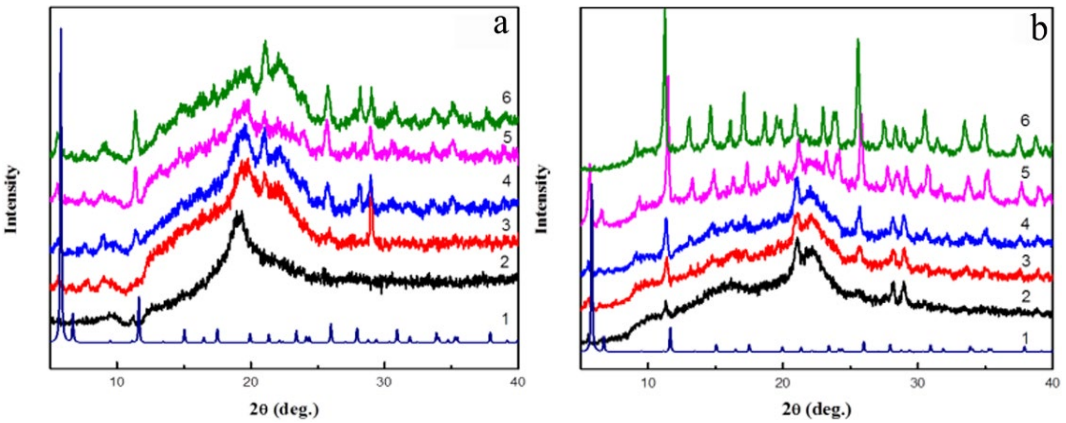

Fig. 1. XRD patterns for simulated MOF-199 (1); PTA@MOF-199-PVA-X (a); PTA@MOF-199-PVP-X (b); X=5%, 10%, 20%, 30%, 50% Wt.% from 2 to 6 respectively).

The morphologies of the as-prepared PTA@MOF-199 NPs has been exhibited in our earlier report [22] and the SEM image was supplied here again (figure 2). The nanoparticles owned a mean diameter of 80-125 nm with uniform morphology. Because of the too small crystal size, all the nanoparticles exhibit irregular shape instead of the typical octahedral appearance of MOF-199 crystals. Additionally, the the desired nanoparticles size ensures the excellent combination of PTA@MOF-199 NPs with the polymeric matrix materials to form smooth and continuous mixed matrix membranes.

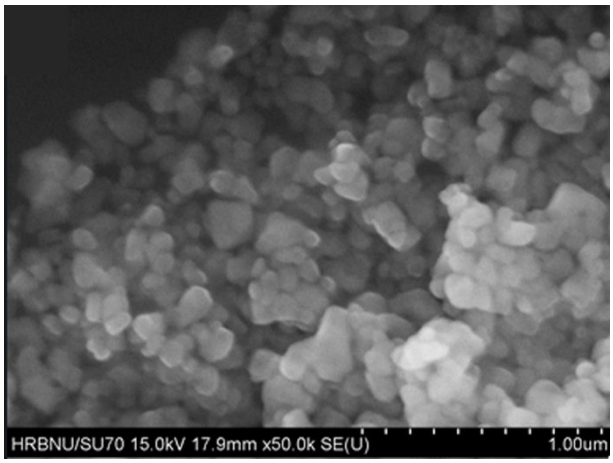

Fig. 2. SEM images of: as-prepared PTA@MOF-199.

The optical images of these hybrid membranes were displayed in figure 3. The thickness and area of all these membranes are similar about 0.01cm and 4.9cm^2 respectively. Generally, these membranes were flat and smooth in the presence of PTA@MOF-199 in all the studied mass percentage ranges. The color of these membranes become darker with the increase of the concentration of PTA@MOF-199 from light blue to deep blue and the light transmission decreased correspondingly. By contrast, these PTA@MOF-199-PVP-X membranes seemed to be more uniform and dense.

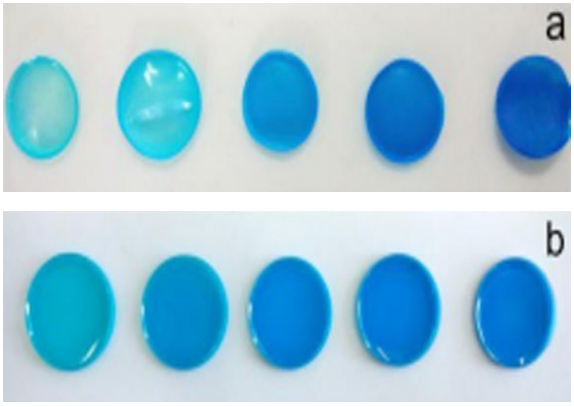

Fig. 3. Optical images of mixed matrix membranes of PTA@MOF-199-PVA-X (a) and PTA@MOF-199-PVP-X. X=5%, 10%, 20%, 30%, 50% Wt.% from left to right respectively.

The corresponding FT-IR data for PAT-MOF-199, PTA@MOF-199-PVA-X and PTA@MOF-199-PVP-X are presented in the region of 4000-400 cm^{-1} (figure 4). For PTA@MOF-199 three peaks at 856 (W-O_b-W), 946 (W-O) and 1056 cm^{-1} (P-O) can be observed, indicating that the Keggin structure is well reserved after immobilizing into the MOF-199 cages[26]. As for PTA@MOF-199-PVA-X and PTA@MOF-199-PVP-X, we could see the C-OH stretching vibration at 1080cm^{-1} and C=O stretching vibration at 1640cm^{-1} respectively.

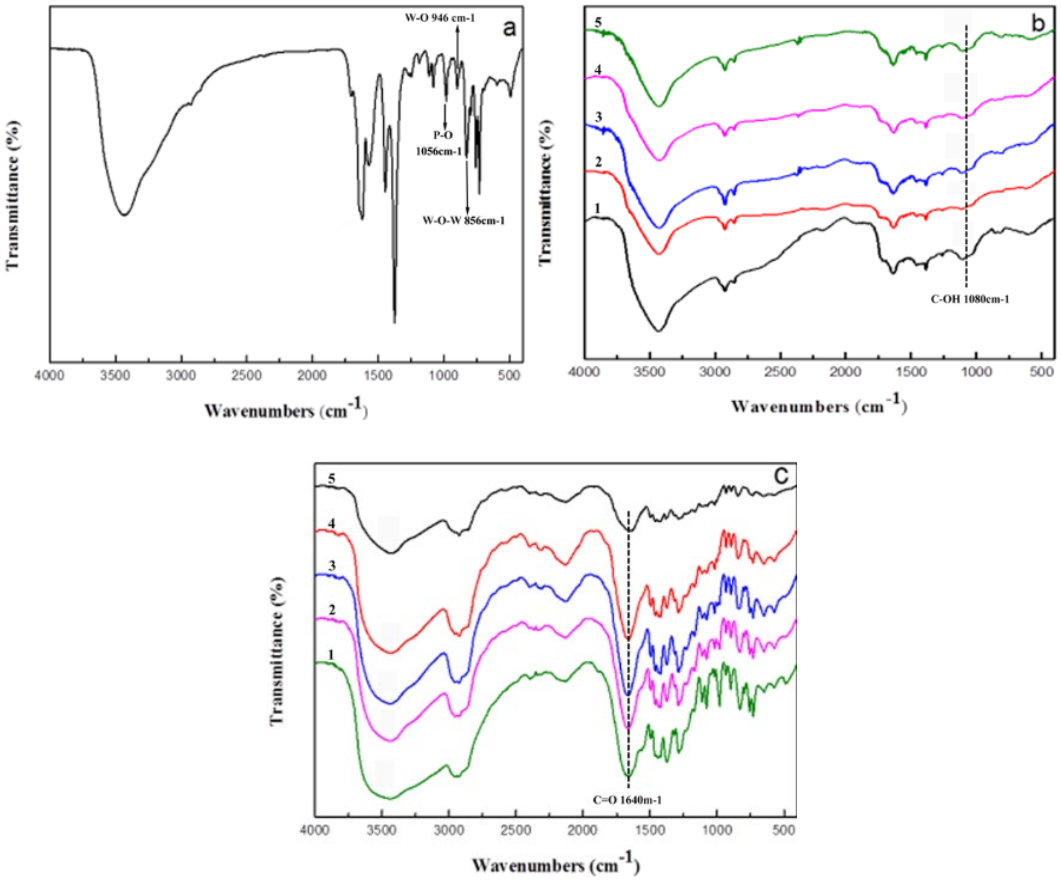

Fig. 4. FT-IR spectra of PTA@MOF-199 (a); PTA@MOF-199-PVA-X (b); PTA@MOF-199-PVP-X(c). X=5%, 10%, 20%, 30%, 50% Wt.% from 1 to 5 respectively.

3.2. Proton conductivity

The influence of the mass percentage of PTA@MOF-199 on the proton-conducting properties of these mixed matrix membranes were evaluated (figure 5a and b) and the corresponding PC values were exhibited in table 1. It is noted that medium loading of PTA@MOF-199 (30% and 10%) gives rise to higher proton conductivity for both the two kinds of mixed matrix membranes at 293K and 98% RH. The results were consistent with a previous report [26]. We speculated the reason might be that when the filling content of PTA@MOF-199 was small, it was hard to form a complete proton transfer channel, but much more nanoparticles in the polymeric matrix materials might engender reunition to produce resistance to the conductivity.

Thus, the appropriate amount of PTA@MOF-199 NPs incorporated into matrix materials is of great importance for achieving the optimum conductivity.

Normally, the proton-conducting properties are influenced greatly by the temperature. In this regard, the temperature-dependent conductivities (σ) of the PTA@MOF-199-PVA-30% and PTA@MOF-199-PVP-10% are implemented at varying temperatures (293-313 K) under 98% RH by alternating current (AC) impedance analysis with a quasi-four-probe method and the result were shown in table 2 and figure 5 c and d. For both the two kinds of membranes, the PC values increased with an elevated temperature. Specifically, when the temperature increased from 293K to 313K, the PC values of PTA@MOF-199-PVA-30% and PTA@MOF-199-PVP-10% were promoted from 4.978×10^{-9} S cm^{-1} to 2.212×10^{-7} S cm^{-1} and 6.110×10^{-9} S cm^{-1} to 1.927×10^{-8} S cm^{-1} respectively indicating that the proton conductivity strongly depend on temperature. Though the PC values were much lower than many other reported proton-conducting membranes [8, 26], in comparation with the undetectable proton conductivity of pure polymeric material membranes under the same condition we could concluded that the dispersed PTA@MOF-199 nanoparticles played an important role in improving the proton conductivity of the mixed matrix membrane.

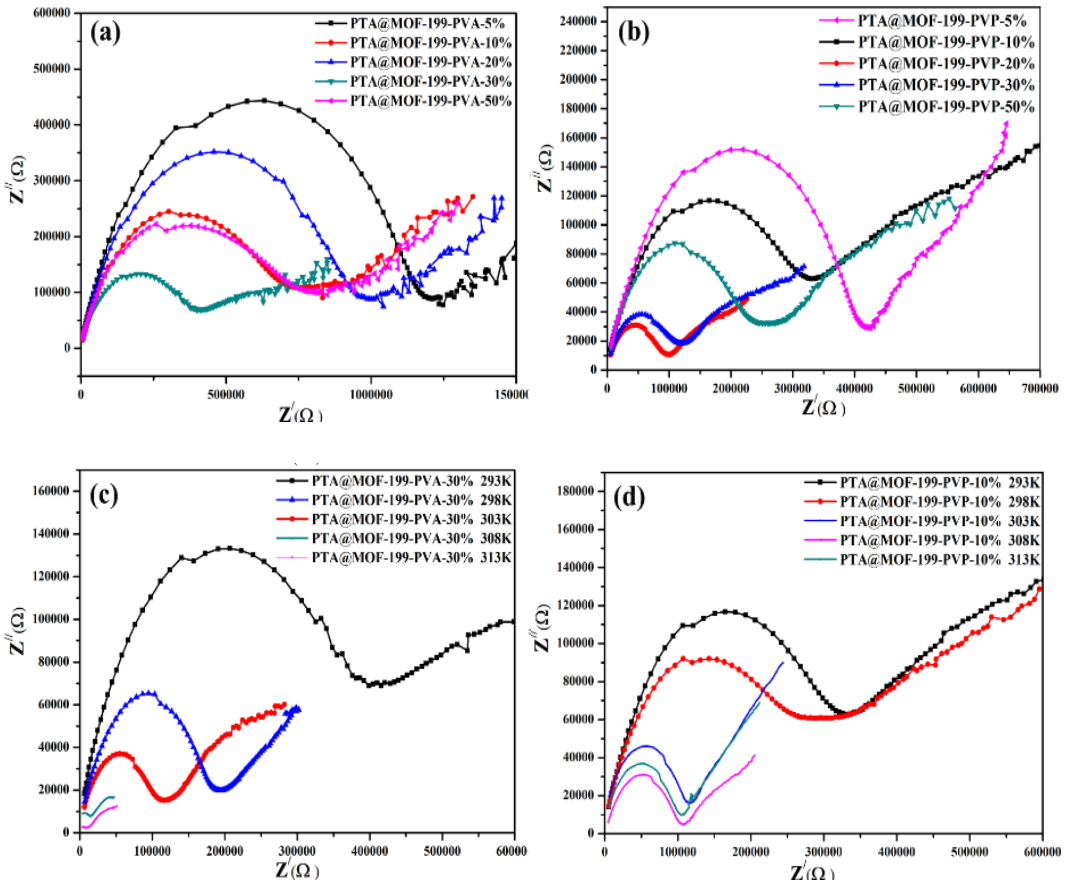

Fig. 5. Nyquist plots of PTA@MOF-199-PVA-X (a) and PTA@MOF-199-PVP-X (b) under 293K and 98%RH; Nyquist plots of PTA@MOF-199-PVA-30% (C) and PTA@MOF-199-PVP-10 (d) under 293K-313K and 98%RH.

Table 1. The PC values of PTA@MOF-199-PVA-X (a) and PTA@MOF-199-PVP-X at 293K and 98%RH condition.

Polymeric matrix materials	PC (S cm^{-1}, T=293K, RH=98%) The mass fraction of PTA@MOF-199				
	5%	10%	20%	30%	50%
PVA	1.695×10^{-9}	2.713×10^{-9}	2.061×10^{-9}	4.978×10^{-9}	2.510×10^{-9}
PVP	4.828×10^{-9}	6.110×10^{-9}	2.036×10^{-8}	1.696×10^{-8}	7.799×10^{-9}

Table 2. The PC values of PTA@MOF-199-PVA-30% and PTA@MOF-199-PVP-10% under 98%RH and different temperatures.

Mixed matrix membranes	PC (S cm^{-1}, RH=98%)				
	293K	298K	303K	308K	313K
PTA@MOF-199-PVA-30%	4.978×10^{-9}	1.054×10^{-8}	1.753×10^{-8}	1.393×10^{-7}	2.212×10^{-7}
PTA@MOF-199-PVP-10%	6.110×10^{-9}	6.926×10^{-9}	1.751×10^{-8}	1.910×10^{-8}	1.927×10^{-8}

4. Conclusions

In summary, the PTA@MOF-199 nanoparticles were prepared by a simple one-pot solvothermal method and the as-prepared nanoparticles were incorporated with two kinds of polymeric matrix materials PVA and PVP as substrates to fabricate a series of proton-conducting mixed matrix membranes with different mass percentage of PTA@MOF-199. The proton conductivity tests results revealed that the reasonable amount of PTA@MOF-199 NPs was vital to achieve the optimum conductivity and the PC properties of these mixed matrix membranes strongly counted on the temperature with PC values increasing with an elevated temperature. In comparation with the undetectable proton conductivity of pure polymeric material membrane, the dispersion of PTA@MOF-199 nanoparticles indeed improved the proton conductivity of the whole membrane. Our work confirmed the POMs functionalized MOFs as promising proton conductive materials and provided a basis for further studies on the fabrication of more PTA@MOFs based proton-conducting membranes.

Acknowledgements

We are grateful to the financial support from the Basic Scientific Research Project of Heilongjiang Province in 2022, China (grant no. 2022-KYYWF-0812).

References

[1] Y. Wang, K.S. Chen, J. Mishler, S.C. Cho, X.C. Adroher, Applied Energy 88(4), 981(2011); https://doi.org/10.1016/j.apenergy.2010.09.030

[2] A. Donnadio, R. Narducci, M. Casciola, F. Marmottini, R. D'Amato, M. Jazestani, H. Chiniforoshan, F. Costantino, Acs Applied Materials & Interfaces 9(48), 42239(2017); https://doi.org/10.1021/acsami.7b14847

[3] E.O. Eren, N. Ozkan, Y. Devrim, International Journal of Hydrogen Energy 47(45), 19690(2022); https://doi.org/10.1016/j.ijhydene.2021.11.045

[4] J. Escorihuela, R. Narducci, V. Compan, F. Costantino, Advanced Materials Interfaces 6(2), 1801146 (2019); https://doi.org/10.1002/admi.201801146

[5] R. Devanathan, Energy & Environmental Science 1(1), 101(2008); https://doi.org/10.1039/b808149m

[6] C. Laberty-Robert, K. Valle, F. Pereira, C. Sanchez, Chemical Society Reviews 40(2), 961(2011); https://doi.org/10.1039/c0cs00144a

[7] J. Escorihuela, J. Olvera-Mancilla, L. Alexandrova, L.F. del Castillo, V. Compan, Polymers 12(9), 1861(2020); https://doi.org/10.3390/polym12091861

[8] E. Bakangura, L. Wu, L. Ge, Z.J. Yang, T.W. Xu, Progress in Polymer Science 57, 103(2016); https://doi.org/10.1016/j.progpolymsci.2015.11.004

[9] J. Lee, O.K. Farha, J. Roberts, K.A. Scheidt, S.T. Nguyen, J.T. Hupp, Chemical Society Reviews 38(5),1450(2009); https://doi.org/10.1039/b807080f

[10] H. Furukawa, K.E. Cordova, M. O'Keeffe, O.M. Yaghi, Science 341(6149), 1230444 (2013); https://doi.org/10.1126/science.1230444

[11] S. Fan, F. Sun, J. Xie, J. Guo, L. Zhang, C. Wang, Q. Pan, G. Zhu, Journal of Materials Chemistry A 1,11438(2013); https://doi.org/10.1039/c3ta11604b

[12] P.L. Zheng, R. Wang, Z.K. Li, Y.R. Li, D.H. Wang, Z.F. Li, X.L. Peng, C.B. Liu, L. Jiang, Q.Y. Liu, High Performance Polymers 33(9), 1035(2021); https://doi.org/10.1177/09540083211011636

[13] S.L. Yang, P.P. Sun, Y.Y. Yuan, C.X. Zhang, Q.L. Wang, Crystengcomm 20(22), 3066(2018); https://doi.org/10.1039/C8CE00476E

[14] F. Yang, H.L. Huang, X.Y. Wang, F. Li, Y.H. Gong, C.L. Zhong, J.R. Li, Crystal Growth & Design 15(12), 5827(2015); https://doi.org/10.1021/acs.cgd.5b01190

[15] F. Yang, G. Xu, Y.B. Dou, B. Wang, H. Zhang, H. Wu, W. Zhou, J.R. Li, B.L. Chen, Nature Energy 2(11), 877(2017); https://doi.org/10.1038/s41560-017-0018-7

[16] A. Münch, F. Mertens, Journal of Materials Chemistry 22(20), 10228(2012); https://doi.org/10.1039/c2jm15596f

[17] S. Bureekaew, S. Horike, M. Higuchi, M. Mizuno, T. Kawamura, D. Tanaka, N. Yanai, S. Kitagawa, Nature Materials 8(10), 831(2009); https://doi.org/10.1038/nmat2526

[18] J.A. Hurd, R. Vaidhyanathan, V. Thangadurai, C.I. Ratcliffe, I.L. Moudrakovski, G.K.H. Shimizu, Nature Chemistry 1(9), 705(2009); https://doi.org/10.1038/nchem.402

[19] W.J. Phang, W.R. Lee, K. Yoo, D.W. Ryu, B. Kim, C.S. Hong, Angewandte Chemie-International Edition 53(32), 8383(2014); https://doi.org/10.1002/anie.201404164

[20] D. Umeyama, S. Horike, M. Inukai, Y. Hijikata, S. Kitagawa, Angewandte Chemie-International Edition 50(49), 11706 (2011); https://doi.org/10.1002/anie.201102997

[21] Z. Rao, B.B. Tang, P.Y. Wu, Acs Applied Materials & Interfaces 9(27), 22597(2017); https://doi.org/10.1021/acsami.7b05969

[22] S.J. Fan, H. Guo, Y.M. Wang, J.H. Liu, Journal of the Indian Chemical Society 99(9), 100579(2022); https://doi.org/10.1016/j.jics.2022.100579

[23] F. Zhang, T.T. Zhang, X.Q. Zou, X.Q. Liang, G.S. Zhu, F.Y. Qu, Solid State Ionics 301, 125(2017); https://doi.org/10.1016/j.ssi.2017.01.022

[24] X. Yan, Y. Meng, Z. Jin, L. Fei, S. Lu, Journal of Membrane Science 368(1-2), 241(2011); https://doi.org/10.1016/j.memsci.2010.11.049

[25] L. Xu, J. Xu, M. Liu, H. Han, H. Ni, L. Ma, Z. Wang, International Journal of Hydrogen Energy 40(22), 7182 (2015); https://doi.org/10.1016/j.ijhydene.2015.02.139

[26] F.L. Wang, C.Y. Liang, J.Y. Tang, F. Zhang, F.Y. Qu, New Journal of Chemistry 44(5), 1912(2020); https://doi.org/10.1039/C9NJ05572J